Structural and optical properties of InP quantum dots grown on GaAs(001)

M. P. F. de Godoy, M. K. K. Nakaema, F. Iikawa, M. J. S. P. Brasil, J. M. J. Lopes, J. R. R. Bortoleto, M. A. Cotta, R. Magalhães-Paniago, M. J. Mörschbächer, and P. F. P. Fichtner

Citation: Journal of Applied Physics **101**, 073508 (2007); doi: 10.1063/1.2718869
View online: http://dx.doi.org/10.1063/1.2718869
View Table of Contents: http://scitation.aip.org/content/aip/journal/jap/101/7?ver=pdfcov
Published by the AIP Publishing

Structural and optical properties of InP quantum dots grown on GaAs(001)

M. P. F. de Godoy, M. K. K. Nakaema, F. Iikawa,[a] M. J. S. P. Brasil, J. M. J. Lopes, J. R. R. Bortoleto, and M. A. Cotta
Instituto de Física "Gleb Wataghin," UNICAMP, Campinas-SP, C.P. 6165, 13083-970, Brazil

R. Magalhães-Paniago
Laboratório Nacional de Luz Síncrotron, C.P. 6192, 13084-971 Campinas-SP, Brazil and Departamento de Física, UFMG, Belo Horizonte-MG, Brazil

M. J. Mörschbächer and P. F. P. Fichtner
Instituto de Física, UFRGS, Porto Alegre-RS, Brazil

(Received 23 May 2006; accepted 15 February 2007; published online 5 April 2007)

We investigated structural and optical properties of type-II InP/GaAs quantum dots using reflection high energy electron diffraction, transmission electron microscopy, atomic force microscopy, grazing incidence x-ray diffraction, and photoluminescence techniques. The InP dots present an efficient optical emission even when they are uncapped, which is attributed to the low surface recombination velocity in InP. We compare the difference in the optical properties between surface free dots, which are not covered by any material, with dots covered by a GaAs capping layer. We observed a bimodal dispersion of the dot size distribution, giving rise to two distinct emission bands. The results also revealed that the strain accumulated in the InP islands is slightly relieved for samples with large InP amounts. An unexpected result is the relatively large blue shift of the emission band from uncapped samples as compared to capped dots. © *2007 American Institute of Physics*. [DOI: 10.1063/1.2718869]

I. INTRODUCTION

Self assembled quantum dots (SAQDs) grown by the Stranski-Krastanov mode have been widely studied in the last decades and it has been demonstrated that they are useful systems for optical applications due to their high quality crystalline structure and interfaces.[1] Several studies have been reported on the applications of SAQDs to optical devices using a large set of semiconductor compounds. There are, however, some points concerning the structural and electronic properties of those structures that are still poorly understood, for instance, the distribution of composition and strain along the dot.

A remarkable characteristic of the InP/GaAs SAQDs is their type II lineup, which provides attractive optical properties for special device applications, such as optical memories.[2] Furthermore, InP/GaAs SAQDs have their optical transition energy in the near-infrared region ($\sim$0.9 μm),[3–5] which is suitable for applications in optical communication devices. Nonetheless, only few works have been reported on their optical and structural properties. Other type II SAQDS are the Si/Ge and the GaSb/GaAs systems, which have optical transitions occurring at larger wavelengths.

In the InP/GaAs SAQDs the electron is confined in the InP material while the hole remains in the GaAs layer close to the interfaces, due to its Coulomb attraction toward the electron. Uncapped SAQDs are normally used to analyze the profile of the dots using atomic force microscopy (AFM). On the other hand, the optical analysis of any SAQDs is usually performed using embedded dots, since the surface states act as efficient non-radiative channels for uncapped dots. Previous studies using uncapped SAQDs have indeed observed weaker photoluminescence (PL) as compared to capped dots on systems such as InAs/GaAs,[6] InGaAs/GaAs,[7] Ge/Si,[8] and InP/InGaP.[9] In contrast, uncapped InP/GaAs SAQDs present an efficient PL emission that allows us to obtain structural and optical properties from the same sample, which is actually a very important advantage when investigating SAQD properties.

We present here the results of a detailed analysis of the structural and optical properties of capped and uncapped InP/GaAs SAQDs using reflection high energy electron diffraction (RHEED), transmission electron microscopy (TEM), atomic force microscopy (AFM), grazing incidence x-ray diffraction (GID) and photoluminescence techniques.

II. EXPERIMENTAL DETAILS

The InP/GaAs SAQDs were grown by chemical beam epitaxy (CBE) on GaAs(001) substrates. After the deoxidation of the GaAs substrate at 600 °C, a 360 nm GaAs buffer layer was grown at 540 °C at a rate of 0.72 μm/h. The sample was then cooled down to 500 °C under As_2 (thermally cracked AsH_3) flux. The InP SAQDs were grown at 0.4 ML/s after a brief interruption with no group V overpressure to prevent exchange processes at the interface. The sample was annealed for 30 s before cooling down. The annealing and cooling processes were performed under a P_2 atmosphere. The nominal volume of InP in monolayers (MLs) units are 4.8 MLs, 5.2 MLs, and 6.0 MLs for samples A, B, and C, respectively, calibrated through the deposition

[a]Electronic mail: iikawa@ifi.unicamp.br

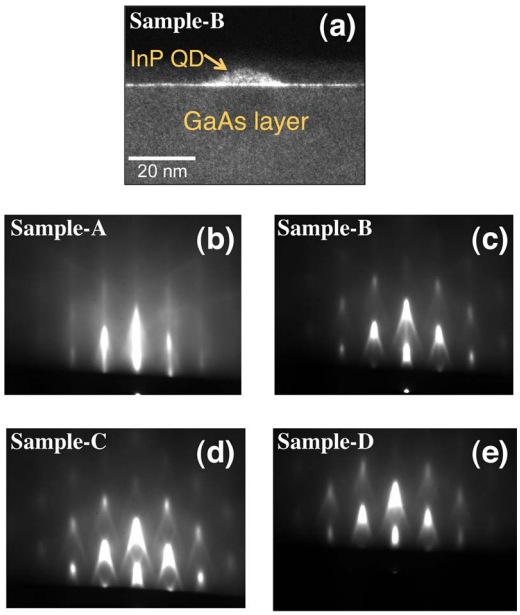

FIG. 1. (a) Cross-sectional TEM dark-field 002 image of sample B. RHEED pattern along the $[1\bar{1}0]$ direction of uncapped InP/GaAs QDs from (b) samples A (4.8 ML), (c) B (5.2 ML), (d) C (6.0 ML), and (e) D (capped with GaAs layer).

time. Sample D was grown under the same conditions as sample B, but it was capped with a 60 nm GaAs layer.

RHEED measurements were performed *in situ* during the growth process. For AFM measurements of the uncapped samples we used the noncontact mode. The cross-sectional TEM analysis was performed using a Jeol JEM-2010 microscope operating at 200 kV. For GID measurements we used a photon energy of 11 keV, which is between the absorption border energies of the In and the Ga elements. For PL measurements, the samples were immersed in liquid He at 2 K and photoexcited with the 488 nm Ar^+ laser line. The luminescence was analyzed using a 1/2 m monochromator and a S1-type photomultiplier.

III. RESULTS AND DISCUSSIONS

A. Structural analysis

The RHEED images measured along the $[1\bar{1}0]$ direction during the growth of the uncapped samples (A, B, and C) are shown in Figs. 1(b)–1(d). All images show typical features related to the formation of quantum dots. The RHEED pattern related to 3D structures from sample A is weak and indicates the beginning of nucleation of the dots. For samples B and C, the chevron-like patterns are more pronounced, indicating the formation of faceting surfaces with an angle of ~20° at the dots, corresponding to the {114} facet. Similarly to previous results on InP/InGaP,[10] those facets are not observed in the RHEED image measured along the [110] direction.

Figure 1(a) shows a cross-sectional TEM image of sample B taken under the dark-field (002) imaging condition. The image shows a lens-like shaped InP QD with a radius of ~12 nm and height of ~3.5 nm from the wetting layer top. The thickness of the wetting layer varies from ~1.0 to ~1.5 nm. The values of the dot size are within the distributions of height and radius of the dots obtained by using AFM measurements presented in Fig. 2. For sample A, when only a small quantity of InP was deposited, the formed structures have a rather small height [Fig. 2(d)], even though they have relatively large radius [Fig. 2(a)]. Those wide and short structures may be interpreted as interface roughnesses or pre-quantum dot formations, which is consistent with the beginning of dot formation observed by using RHEED. When the InP deposition is slightly increased (sample B), the dot mean-height increases [Fig. 2(e)] showing a tendency of a bimodal-like distribution, while the radius distribution shifts to smaller values [Fig. 2(b)]. With a further increase in the InP amount (sample C), the height distribution becomes markedly larger [Fig. 2(f)] and shows the formation of much higher dots. The radius distribution for sample C [Fig. 2(c)] remains, however, similar to sample B [Fig. 2(b)]. The density of dots increases as the deposition time increases. We obtained 0.6, 1.2, and 4.5×10^{10} cm^{-2} for samples A, B, and C, respectively. Figures 2(g)–2(i) also show the evolution of the height versus radius distribution for our samples. A starting flat-like distribution obtained for the sample with the smallest InP amount [Fig. 2(g)] becomes more spread out as the InP quantity increases [Fig. 2(h)], evolving to a distinct linear correlation between height and radius [Fig. 2(i)], where the dots maintain a radius/height ratio almost constant.

The results of GID (θ-2θ) measurements for the uncapped samples are presented in Fig. 3. The GID measurements were performed using the same x-ray beam incidence angle (~0.2°) and other experimental conditions for all samples. The diffraction intensity is plotted as a function of the variation of the in-plane lattice parameter a relative to the GaAs substrate (a_{sub}=5.6533 Å), $(a-a_{sub})/a_{sub}$. The dominant peak at $(a-a_{sub})/a_{sub}=0$ (see Fig. 3) corresponds to the $(2\bar{2}0)$ reflection from the GaAs substrate, but it also includes the diffraction from the commensurate InP material present in the sample. We observe a tail around the dominant peak, mainly on its right side (corresponding to larger lattice parameters). The intensity of the tail increases when the amount of InP is increased. For sample A, the tail intensity is rather weak, while for samples B and C the tail becomes very pronounced revealing a maximum at $(a-a_{sub})/a_{sub}\sim0.006$. Those results indicate that when InP QDs higher than ~1.5 nm (sample B and C) are formed, the samples present regions with in-plane lattice parameters larger than the GaAs substrate, but still smaller than bulk InP $[(a-a_{sub})/a_{sub}=0.036]$. The compressive strain on large InP QDs is thus partially relieved as observed in previous works on InAs/GaAs[11,12] and Ge/Si.[13,14]

B. Optical analysis

Figure 4 shows the PL spectra from our samples under identical excitation conditions. All samples present a strong emission peak at ~1.49 eV due to the band-acceptor and donor-acceptor recombinations in the GaAs layer. The highest energy band below the GaAs emission is attributed to the optical emission from the WL, while the low energy bands are attributed to InP QDs. The PL spectra from sample A is dominated by the optical emission from the WL, with a weak

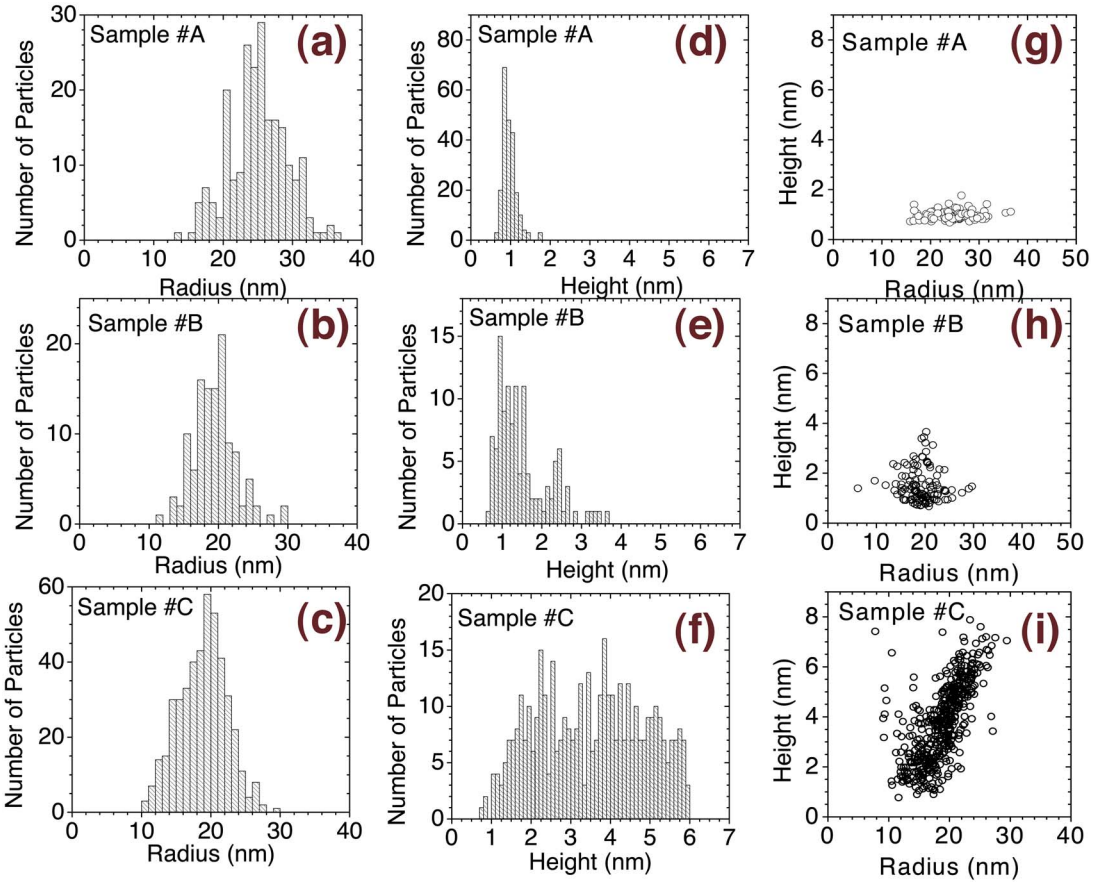

FIG. 2. Histograms of the radius (a)–(c) and the height (d)–(f) and height and radius distributions (g)–(i) of the SAQDs obtained from the AFM image measured in 2×2 μm^2 in sample A and 1×1 μm^2 in samples B and C.

shoulder at the low energy side, which is attributed to the recombination from the pre-dot structures, as previously. As the InP volume increases (sample B and C), the recombination intensity from the InP QDs increases and dominates the WL optical emission. Furthermore, the WL emission bands from those samples are shifted to lower energies. This indicates that the thickness of the WL increases during the formation of the "actual" QDs, since the PL peak energy of the WL is mainly defined by its thickness. Samples B and C also present two low energy bands below the WL emission, both associated with InP QDs. The observation of two emission bands, named here as QD1 and QD2, is in agreement with the bimodal QD height distribution observed by AFM (Fig. 2). We remark that the partial relief of strain observed for uncapped samples with larger QDs can contribute to a larger emission energy dispersion, since the strain relief is more significant for larger QDs and it should result in a decrease of the transition energy, due to a decrease of the gap energy.

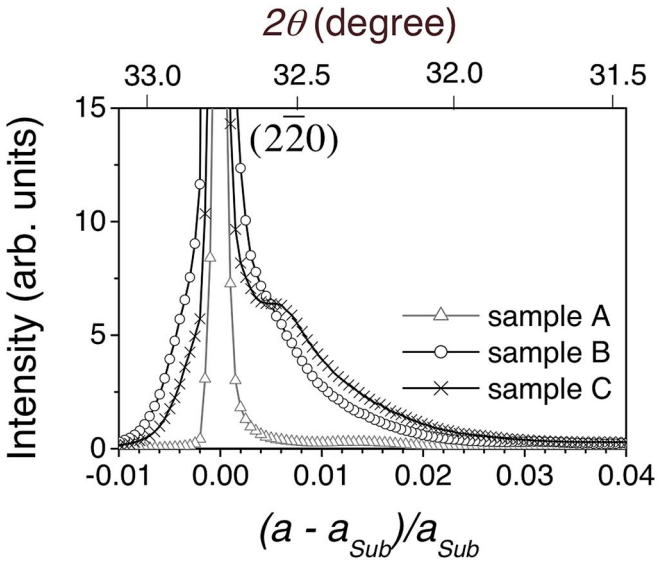

FIG. 3. Grazing incidence x-ray diffraction patterns measured for uncapped samples A (4.8 MLs), B (5.2 MLs), and C (6.0 MLs). The superior horizontal axis is the nonlinear scale of 2θ.

Surprisingly, the PL spectra from samples B and C are very similar in both the presence of two emission bands associated to dots (QD1 and QD2) and their energy positions. The QD height distribution is, nevertheless, quite different for those two samples. The bimodal characteristic is no longer discerned in sample C, which presents significantly thicker QDs, with a large amount of QDs with heights larger than ~3.5 nm (Fig. 2), while almost no QDs are observed in sample B with such heights. We would thus expect some optical emission at lower energies for sample C, remarking that the photomultiplier used is rather sensitive up to ~1.1 μm (~1.13 eV). This absence can be related to an increase of defects that favors nonradiative recombination on thicker QDs.

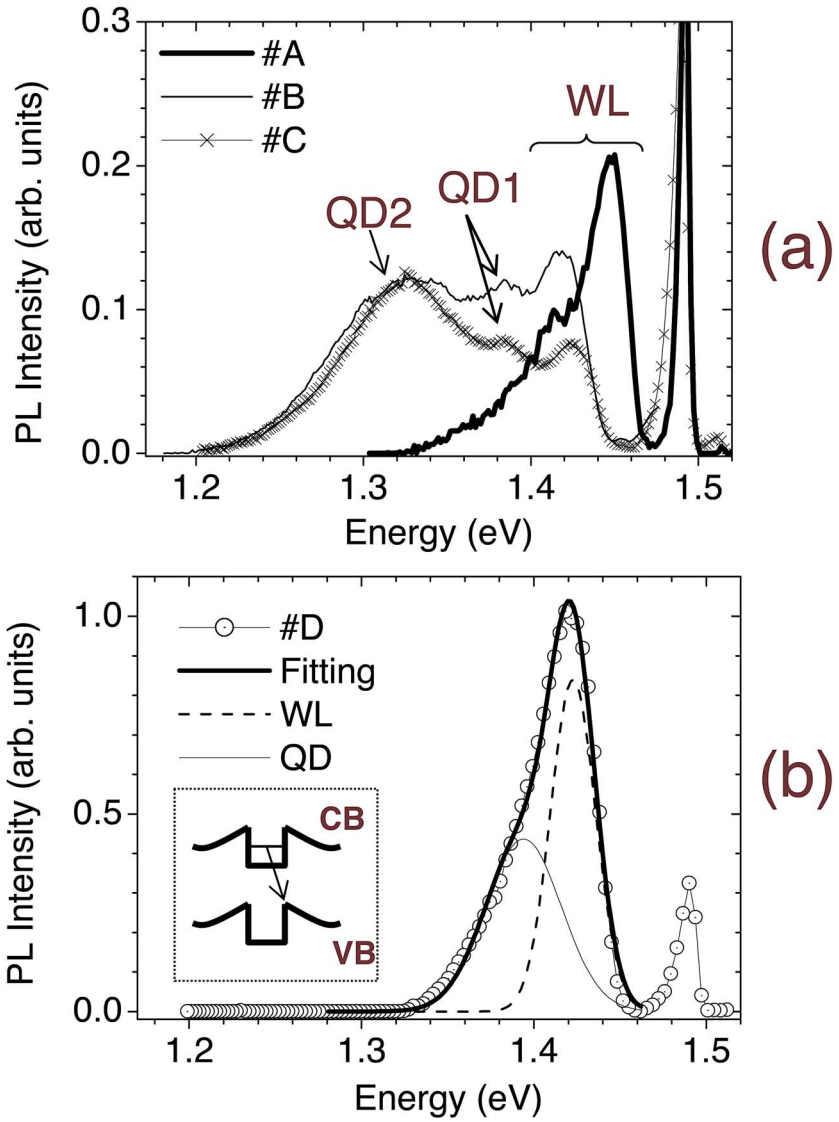

FIG. 4. Photoluminescence spectra measured at 2 K and laser power of 0.1 mW from (a) uncapped (A, B, and C) and (b) capped (D) SAQDs. All spectra were corrected with the spectral response of the photomultiplier. The inset shows the diagram of the potential profile of type-II InP/GaAs QDs.

We observed that the optical efficiency of the uncapped samples is smaller than that from the capped one by only a factor ~6. The efficient optical emission in uncapped QDs has also been observed in a previous work for InP/InGaP SAQDS.[9] Surface states usually work as efficient nonradiative channels for the photocreated carriers. The surface recombination velocity for In-based compounds such as InP,[15–18] is significantly smaller than that for GaAs.[15] This explains the efficient optical emission observed from uncapped InP QDs. We point out, however, that the effect of surface state, although relatively weak as compared to As-based dots, should be more significant for thinner layers such as the WL when compared to thick layers such as the QDs. We thus expect to obtain a weaker emission intensity from the WL relative to the QDs for uncapped samples as compared to the capped samples for which the surface states do not play any role in the InP emission.

The PL spectrum from the capped sample (sample D) shown in Fig. 4(b) is indeed remarkably different from sample B, which was grown under the same conditions but without the capping layer. It presents a single asymmetric emission band, whose intensity is even larger than the emission band at ~1.49 eV from shallow acceptor states in the GaAs layer. The asymmetry indicates that this band includes the recombination from both the WL and the QDs, which are not resolved. In Fig. 4(b) we also plotted the curves obtained by fitting the PL emission with two Gaussian functions that should represent thus the QD and WL emission bands. The peak energy of the WL emission band is similar to that from sample B, but we only observed a single QD emission band whose peak energy is blue shifted as compared to the higher energy QD emission band (QD1). That explains why those two bands are not resolved anymore for sample D, while they are clearly resolved for sample B. The partial relief of the compressive strain of the InP QDs observed for uncapped samples should be less significant for capped samples, due to the thick GaAs cap layer. This can contribute to a blue shift of the optical emission from the QDs of the capped sample as compared to the uncapped ones, reducing the energy separation between the QDs and WL optical emission bands. The blue shift can also been attributed to a reduction of the QD height as the cover layer thickness is increased.[6] Similar results have been observed for other systems such as InAs/GaAs,[6] InGaAs/GaAs,[7] and InP/InGaP.[9] We should also

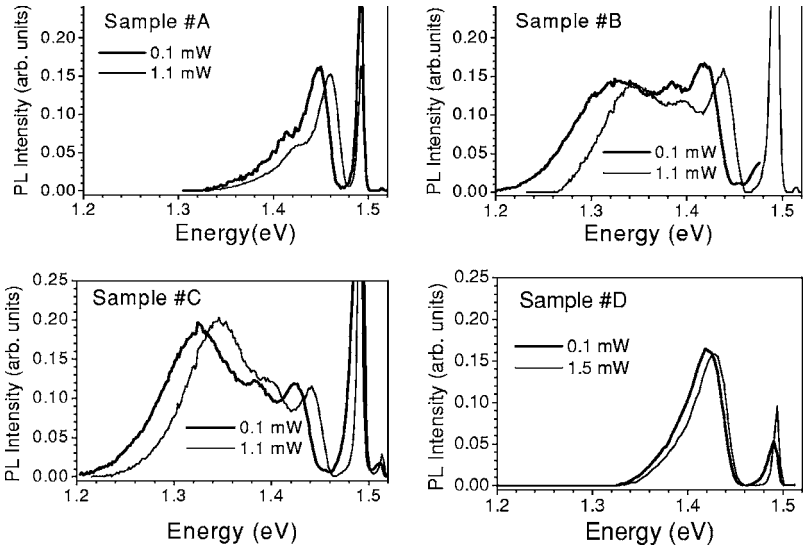

FIG. 5. Normalized photoluminescence spectra of uncapped InP/GaAs QD samples A (4.8 ML), B (5.2 ML), C (6.0 ML), and capped D (5.2 ML).

consider the contribution of the intermixing at the interfaces, which results in a blue shift. However, a detailed information of the effect of the capping layer on the optical emission of the QDs is still under progress.

Figure 5 shows the normalized PL spectra for two laser intensities for our samples. The increase of the excitation intensity results in a blue shift of the optical emission bands for all samples, but the energy shift is noticeably larger for uncapped samples as compared to the capped one. For the capped sample, the energy shift is ~5 meV for QDs and WL, while for uncapped samples, it is of the order of 10 meV. The characteristic blue shift from type II emission bands for increasing excitation intensities has been attributed to different origins for the QD and the WL.[5,19] The former is attributed to the appearance of additional emissions related to the many particle complexes, such as trions and multiexcitons. These have rather large emission energies due to the reduced attractive Coulomb interaction as compared to the repulsive one for complexes with more than two particles in type II structures. The latter is attributed to the variation of the triangle-like electrostatic potential profile along the growth direction as a function of the carrier concentration.

It is important to point out that the optical transition in our samples occurs between electrons confined in the InP layer (WL and QDs) and holes at the GaAs layers. The hole is localized close to the InP/GaAs interface solely by the Coulomb interaction. In the case of the capped sample, the holes may remain in the GaAs layers on both sides of the InP layer, while for uncapped samples the holes can only remain at the GaAs layer under the InP layer. The larger charge concentration for the uncapped samples may be responsible for a larger blue shift for both QD and the WL emission from those samples when compared to the capped one as the carrier density increases. An additional effect that may be considered is the formation of an alloy at the QD interfaces, mainly at the top side, which can significantly change the potential profile at the interfaces of capped versus uncapped samples. The presence of an As-based alloy, such as InGaAs and InAsP, should result in a deeper potential well, for both electrons and holes, generating an additional confinement potential for holes. This effect should also increase the electron-hole attraction, as compared to the repulsion terms for the capped sample and, therefore, decreasing the transition energy of the type-II exciton complexes.

IV. CONCLUSIONS

We investigated the structural and optical properties of InP/GaAs SAQDs of uncapped and capped samples using different experimental techniques. The combination of structural and optical results for a given sample is very useful to analyze the properties of those nanostructures. We observed a bimodal QD distribution, which is consistent with two resolved emission bands from QDs observed in the photoluminescence spectra. The photoluminescence spectra and their behavior with the excitation intensity from uncapped and capped samples are rather distinct. They can be attributed to a combination of several factors which affects uncapped and capped QDs differently: nonradiative recombination of the surface states, strain relief of the QDs, charge distribution and the alloy formation at the interfaces. We presented important structural and optical results that can be useful for the fabrication of the InP/GaAs structures for device applications.

ACKNOWLEDGMENTS

The authors thank J. H. Clerici and K. O. Vicaro for helpful support in AFM measurements, Milton M. Tanabe for technical support, CME-UFRGS for TEM measurements, and the Brazilian Synchrotron Laboratory (Laboratório Nacional de Luz Sincrotron—LNLS) for GID measurements. We also acknowledge the financial support from CAPES, CNPq, FAPESP, and FAEP.

[1] P. M. Petroff, A. Lorke, and A. Imomoglu, Phys. Today **54**, 46 (2001), and references therein.
[2] M. C. Böedefeld, R. J. Warburton, K. Kanai, J. P. Kotthaus, G. Medeiros-Ribeiro, and P. M. Petroff, Appl. Phys. Lett. **74**, 1839 (1999).
[3] B. Wang and S.-J. Chua, Appl. Phys. Lett. **78**, 628 (2001).
[4] G. Medeiros-Ribeiro, R. L. Maltez, A. A. Benussi, D. Ugarte, and W. de Carvalho, Jr., J. Appl. Phys. **89**, 6548 (2001).
[5] M. K. K. Nakaema, F. Iikawa, M. J. S. P. Brasil, E. Ribeiro, G. Medeiros-

Ribeiro, W. Carvalho, Jr., M. Z. Maialle, and M. H. Degani, Appl. Phys. Lett. **81**, 2743 (2002).
[6]F. Ferdos, S. Wang, Y. Wei, A. Larsson, M. Sadeghi, and Q. Zhao, Appl. Phys. Lett. **81**, 1195 (2002).
[7]H. Saito, K. Nishi, and S. Sugou, Appl. Phys. Lett. **73**, 2742 (1998).
[8]M. Larsson, A. Elfving, P. O. Holtz, G. V. Hansson, and W.-X. Ni, Appl. Phys. Lett. **82**, 4785 (2003).
[9]M.-E. Pistol, N. Carlsson, C. Persson, W. Seifert, and L. Samuelson, Appl. Phys. Lett. **67**, 1438 (1995).
[10]J. R. R. Bortoleto, H. R. Gutiérrez, M. A. Cotta, and J. Bettini, Appl. Phys. Lett. **87**, 013105 (2005).
[11]M. Grundmann, O. Stier, and D. Bimberg, Phys. Rev. B **52**, 11969 (1995).
[12]C. Pryor, J. Kim, L. W. Wang, A. J. Williamson, and A. Zunger, Appl. Phys. Lett. **83**, 2548 (1998).
[13]O. G. Schmidt, K. Eberl, and Y. Rau, Phys. Rev. B **62**, 16715 (2000).
[14]Y. Kikuchi, H. Sugii, and K. Shintani, Appl. Phys. Lett. **89**, 1191 (2001).
[15]H. G. Casey, Jr. and E. Buehler, Appl. Phys. Lett. **30**, 247 (1977).
[16]K. T. Tsen, G. Halama, O. F. Sankey, S.-C. Tsen, and H. Morkoç, Phys. Rev. B **40**, 8103 (1989).
[17]K. Tai, R. Hayes, S. L. McCall, and W. T. Tsang, Appl. Phys. Lett. **53**, 302 (1988).
[18]E. Yablonovitch, R. Bhat, C. E. Zah, T. J. Gmitter, and M. A. Koza, Appl. Phys. Lett. **60**, 371 (1992).
[19]L. Müller-Kirsch, R. Heitz, A. Schliwa, O. Stier, D. Bimberg, H. Kirmse, and W. Neuman, Appl. Phys. Lett. **78**, 1418 (2001).